Electronic Supplementary Material (ESI) for Journal of Materials Chemistry C.

Supporting Information

Increasing resonance energy transfer upon dilution:

a counterintuitive observation in CTAB micelles

Andrea Delledonne [a], Judit Morlà[b,c] ,Mattia Anzola[a], Francesco Bertocchi [a], Guillem Vargas-Nadal[b,c], Mariana Köber[c,b], Cristina Sissa [a] , Nora Ventosa[b,c,*], and Anna Painelli [a,*]

[a] Dipartimento di Scienze Chimiche, della Vita e della Sostenibilità Ambientale, Università di Parma, Parco Area delle Scienze 17A, 43124, Parma, Italy

[b] Institut Ciencia dels Materials de Barcelona (ICMAB-CSIC), Campus UAB, 08193 Cerdanyola, Spain; [c] Centro de Investigación Biomédica en Red CIBER-BBN, Barcelona, Spain;

*Corresponding authors

1. Composition of the studied formulations

		Dye concentration		CTAB concentration (mM)	Volume fraction of EtOH	Volume fraction of H_2O
		DiI (μM)	DiD (μM)			
EtOH/H_2O	DiI in EtOH/H_2O	20	-	-	30 %	70 %
	DiD in EtOH/H_2O	-	20	-	30 %	70 %
CTAB 0.5 mM	DiI in CTAB 0.5 mM	0.8	-	0.5	< 1 %	~ 100 %
	DiD in CTAB 0.5 mM	-	0.8	0.5	< 1 %	~ 100 %
	DiI +DiD in CTAB 0.5 mM	0.4	0.4	0.5	< 1%	~ 100 %
CTAB 7 mM	DiI in CTAB 7 mM	11	-	7	11 %	89 %
	DiD in CTAB 7 mM	-	11	7	11 %	89 %
	DiI +DiD in CTAB 7 mM	5.5	5.5	7	11 %	89 %

Table S1. Composition of the studied formulations, details about the preparation can be found in the experimental section.

2. DiI and DiD aggregates in water-ethanol mixtures

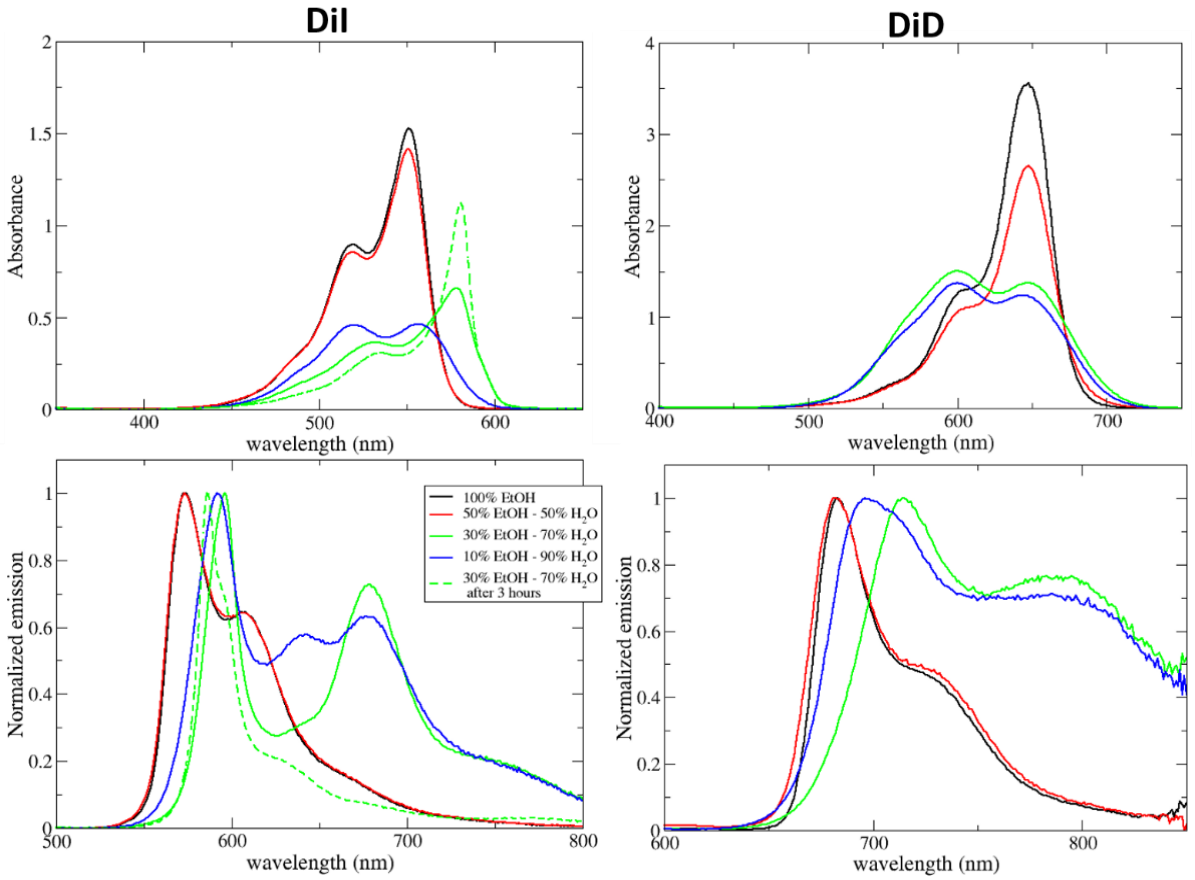

Figure S1: Absorption (top) and emission (bottom) spectra of DiI (left) and DiD (right) in different water-ethanol mixtures: black 100% ethanol; red=50% ethanol; green= 30% ethanol; blue= 10% ethanol (volume percentages). Clear aggregation features appear when water volumes exceed ethanol volumes. Spectra of aggregates change with time, mainly in the first 3 hours after preparation, as shown in the figure for aggregates in 30% ethanol mixtures.

Table S2. Dynamic Light Scattering (DLS) results (cumulant analysis) of DiI and DiD in different water-ethanol mixtures. For aggregates in 30% ethanol mixtures, the quality of data is satisfactory. For the aggregates in the 10% ethanol mixture data are less reliable, due to the high polydispersity and/or the presence of sedimenting particles.

Sample	Z-Average* [nm]	Z std deviation	PdI	PdI std deviation
DiI in 30% EtOH – 70% H_2O	68	0.57	0.406	0.035
DiI in 30% EtOH – 70% H_2O after3 hours	83	1.09	0.438	0.023
DiI in 10% EtOH – 90% H_2O	3291	5104	0.622	0.288
DiD in 30% EtOH – 70% H_2O	29	0.36	0.267	0.017

*Average of 3 measurements for 30% ethanol mixtures; average of 4 measurements for the 10% ethanol mixture.

3. Spectroscopic characterization of CTAB micelles loaded with DiI or DiD

Table S3. Exponential components analysis obtained from reconvolution fits of emission decays.

	t_1(ns)	B_1	t_2(ns)	B_2	<t> (ns)*	χ^2
DiI CTAB 1 mM	0.48	0.017	1.96	0.0002	0.55	0.99
DiI CTAB 0.5 mM	0.26	0.027	1.91	0.0001	0.30	1.2
DiD CTAB 1 mM	0.92	0.0063	1.60	0.0057	1.34	1.1
DiD CTAB 0.5 mM	0.56	0.016	1.96	0.0003	0.65	0.97

**Average lifetime:* $\langle t \rangle = \frac{B_1 t_1^2 + B_2 t_2^2}{B_1 t_1 + B_2 t_2}$

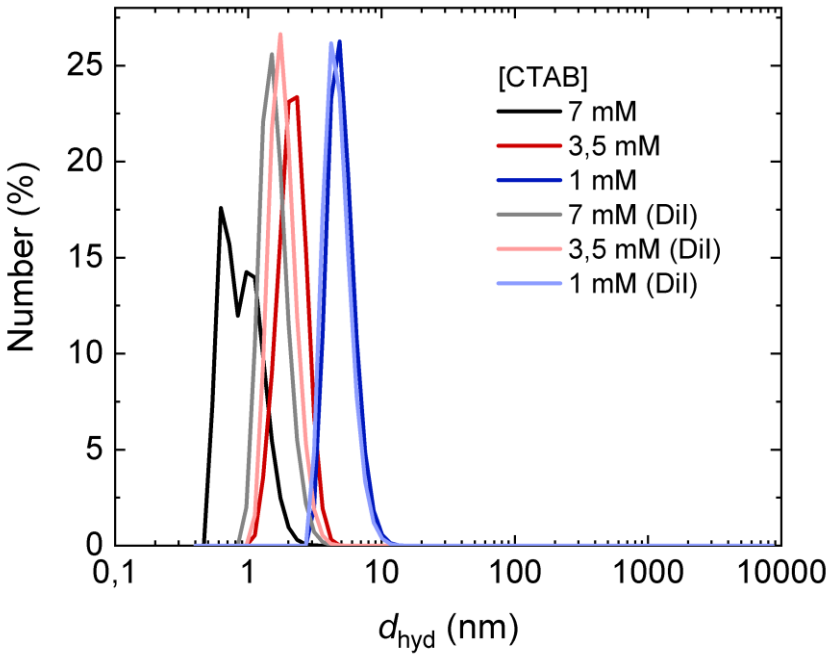

Figure S2. Number of particles vs size distributions obtained from the analysis of DLS data for formulations at different CTAB concentrations with and without DiI. Results demonstrate the presence of micelles with mean diameters in the range of 2-5 nm, in line with literature data.[1,2] At larger CTAB concentrations (7 mM) the estimated size is probably reduced due to artifacts from multiple scattering events.[3] The number size distribution is calculated assuming for the micelles the physical parameters of polystyrene latex: RI=1.590, A=0.010.

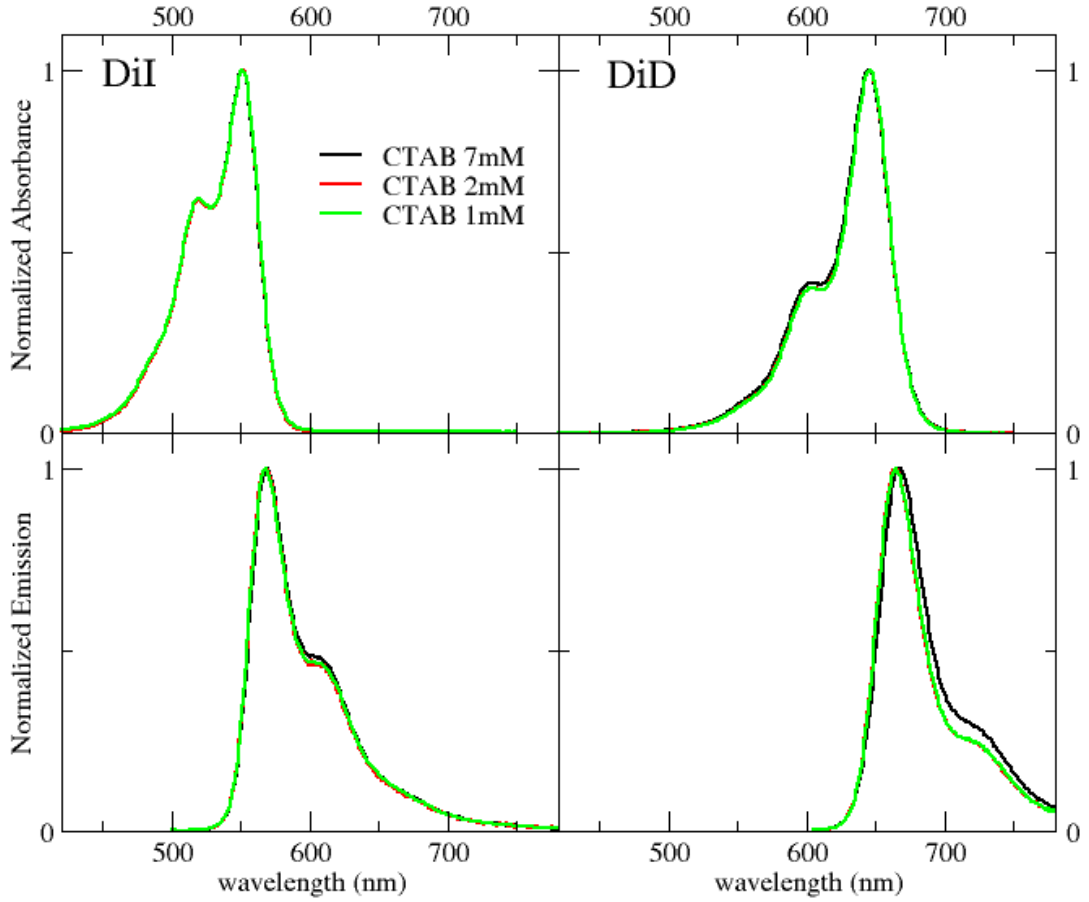

Figure S3: Absorption and emission of DiI and DiD in micelles at different concentrations, for CTAB concentration above the CMC (the relative concentration of chromophores and CTAB is constant). To minimize inner filter effects, emission spectra are collected in a cuvette with 1.5 mm optical path.

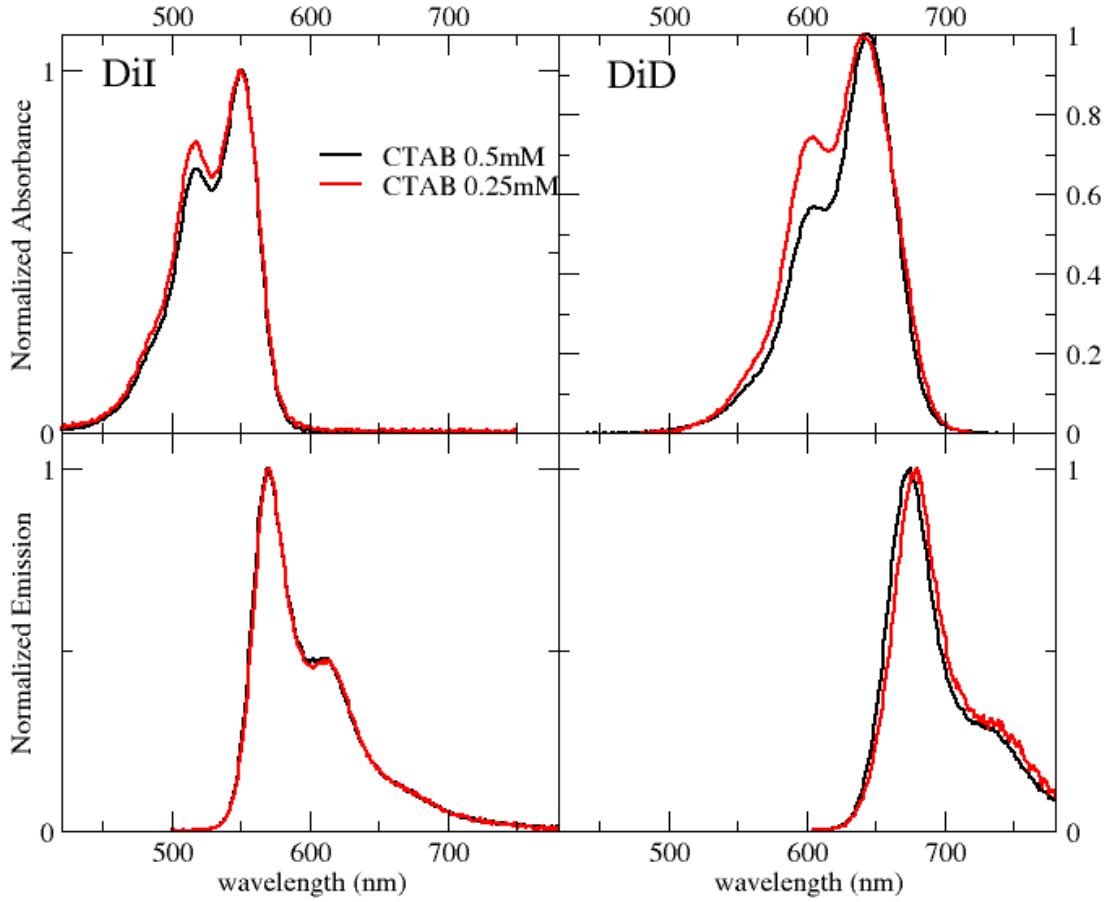

Figure S4: Absorption (top) and emission spectra (bottom) of DiI and DiD in water with CTAB concentrations below and above the CMC (the relative concentration of chromophores and CTAB is constant).

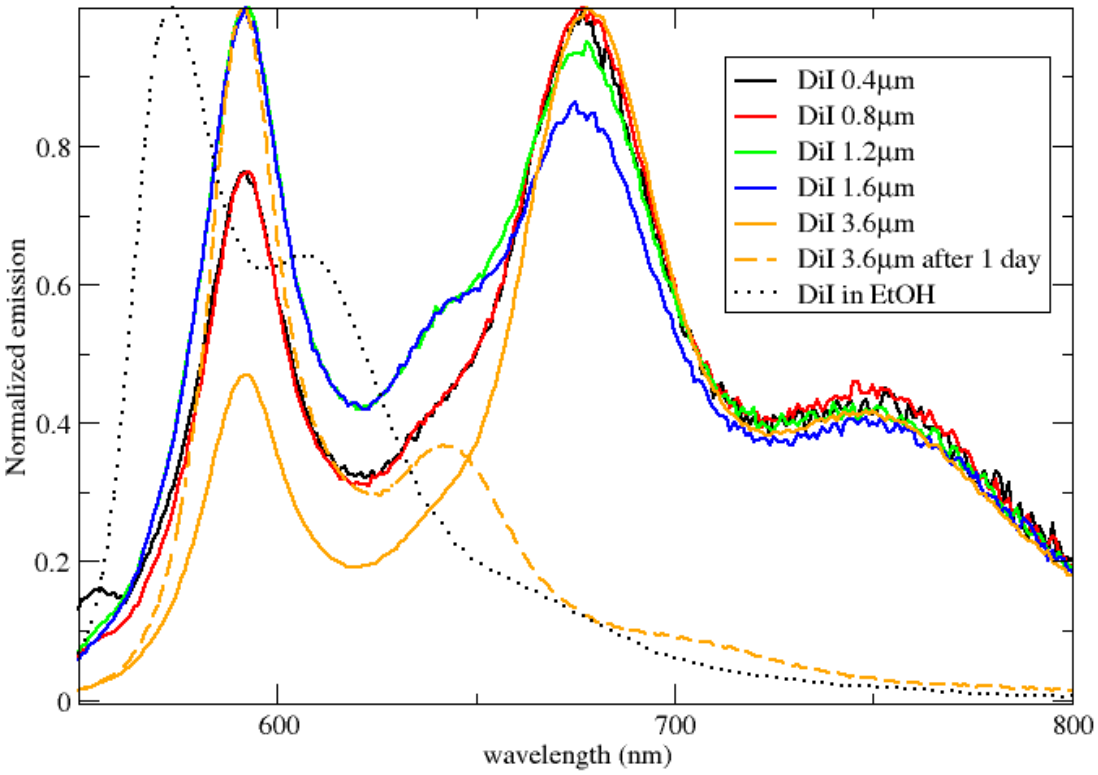

Figure S5: Emission spectra of DiI added to a solution of CTAB 0.5mM. The legend lists the overall DiI concentration. The spectrum collected in EtOH is shown for comparison. Emission spectra compare well with emission spectra of DiI in ethanol/water mixtures (Figure S1).

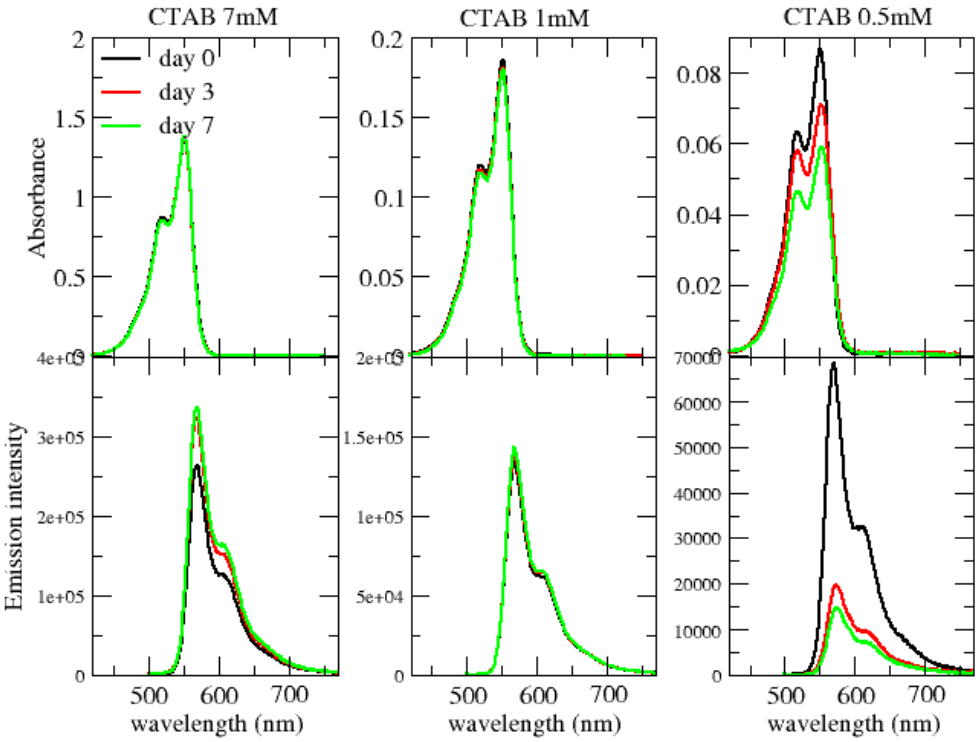

Figure S6: Time evolution of absorption and emission spectra of DiI in water in the presence of CTAB. The relative dye/CTAB concentration is the same in all samples.

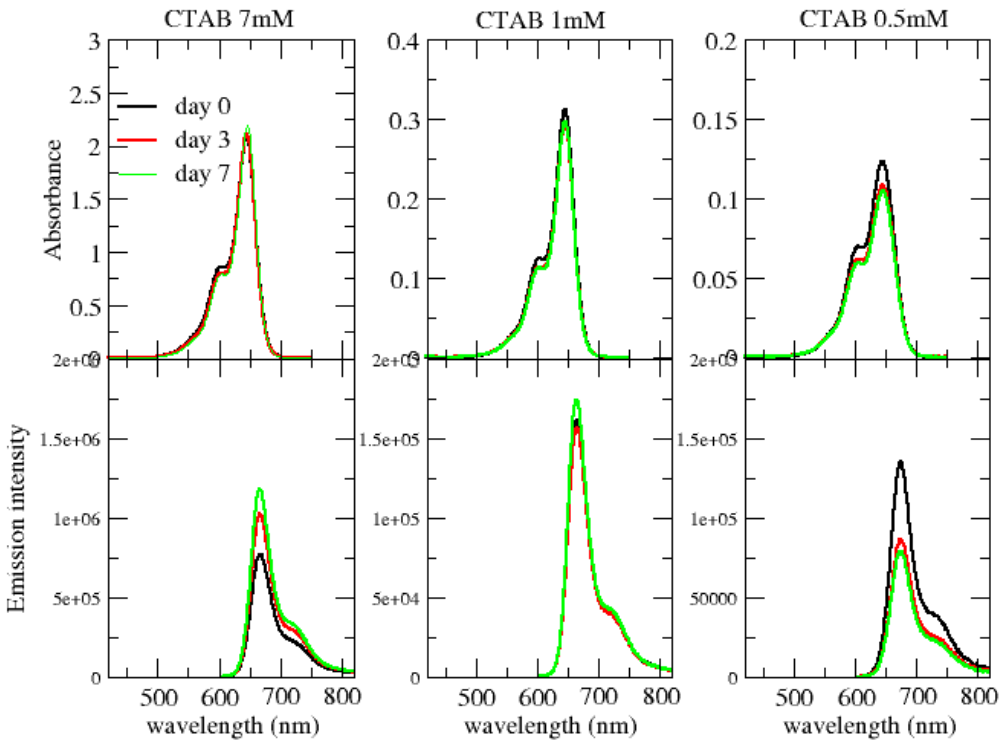

Figure S7: Time evolution of absorption and emission spectra of DiD in water in the presence of CTAB. The relative dye/CTAB concentration is the same in all samples.

3. Spectroscopic characterization of CTAB micelles loaded with DiI and DiD

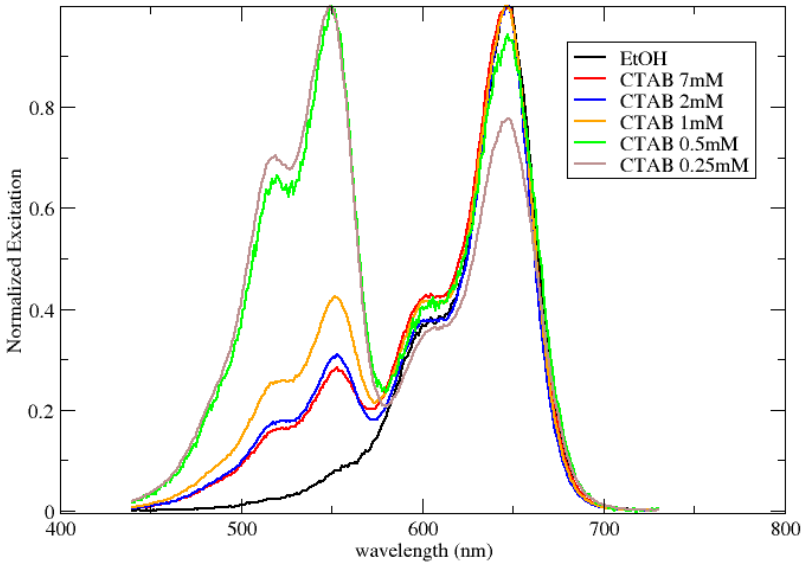

Figure S8: Excitation spectra of micelles loaded with both DiI and DiD, collected at 750 nm (emission of the energy acceptor). To minimize inner filter effects, for suspensions at 7 and 2 mM, spectra are collected using a cuvette with 1.5 mm optical path.

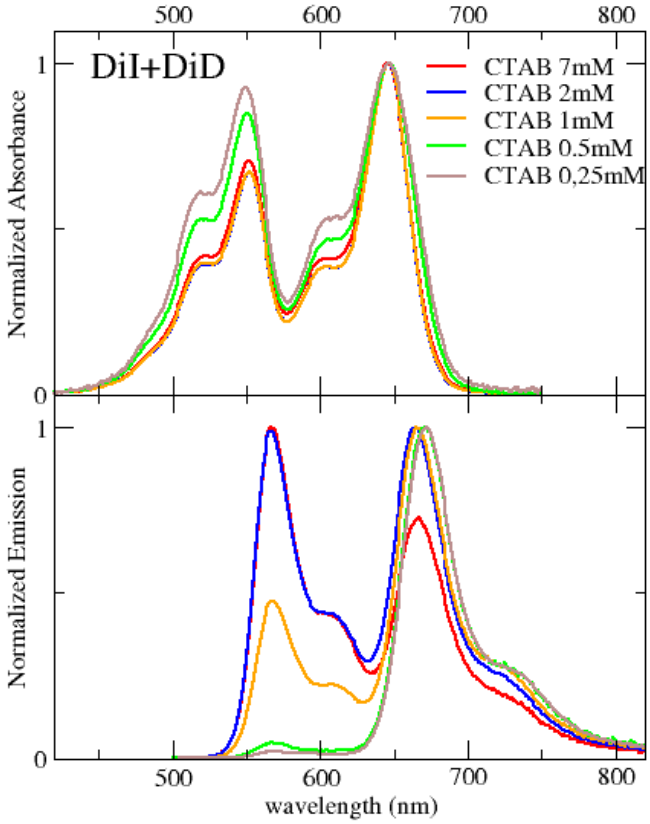

Figure S9: Absorption and emission spectra of micelles loaded with both DiI and DiD. Emission spectra were collected exciting the sample at 495 nm (where the absorption of DiD is negligible). To minimize inner filter effects, for suspensions at 7 and 2 mM, spectra are collected using a cuvette with 1.5 mm optical path.

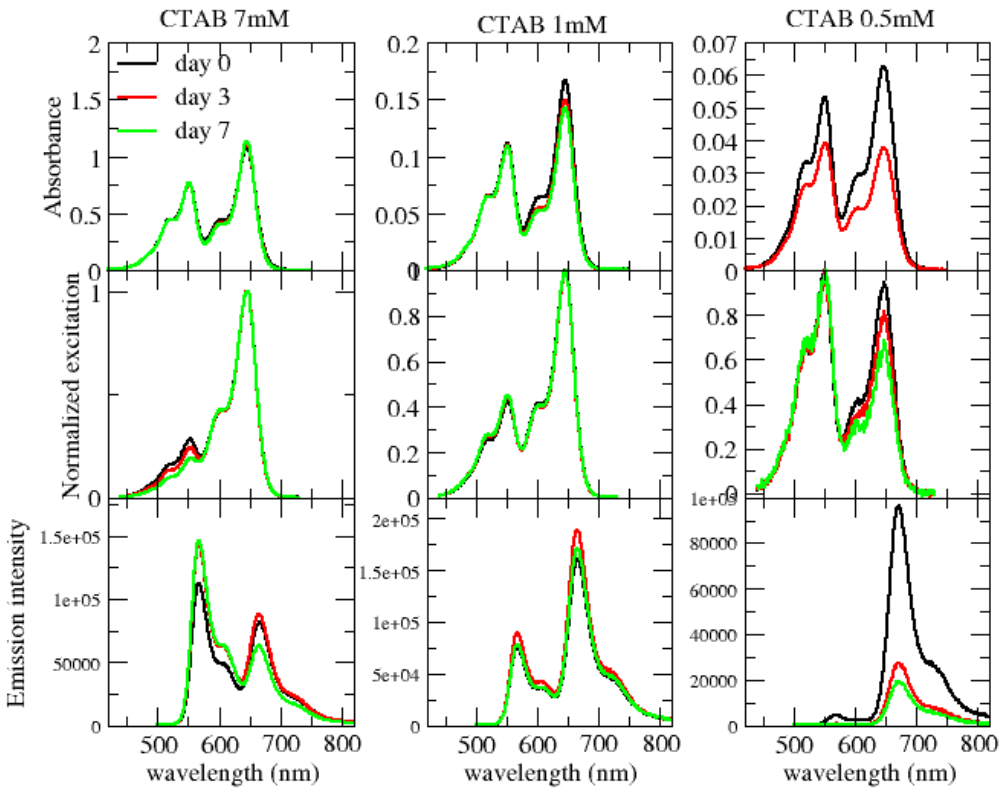

Figure S10: Stability over time of micelles loaded with both DiI and DiD for different CTAB concentration (7 mM and 1 mM). CTAB 0.5 mM is under the CMC, thus CTAB is no longer forming stable micelles.

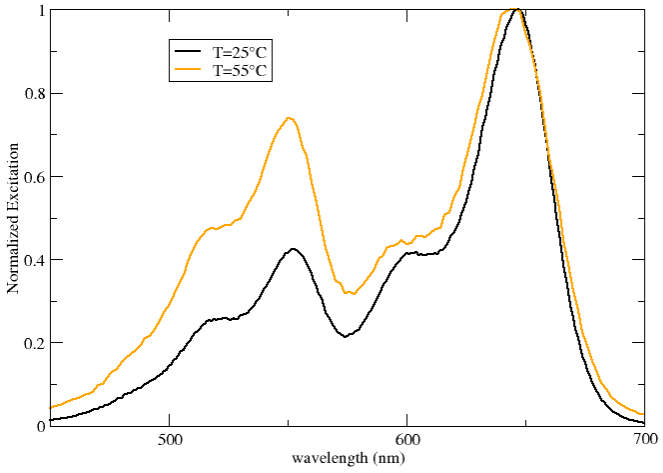

Figure S11: Excitation spectra of micelles loaded with both DiI and DiD at two different temperatures (concentration of CTAB: 1mM). Emitted light is collected at 750nm, where only the energy acceptor DiD is emitting. The increase of the signal observed at high temperature in the region where the energy donor DiI absorbs, demonstrates increased FRET efficiency.

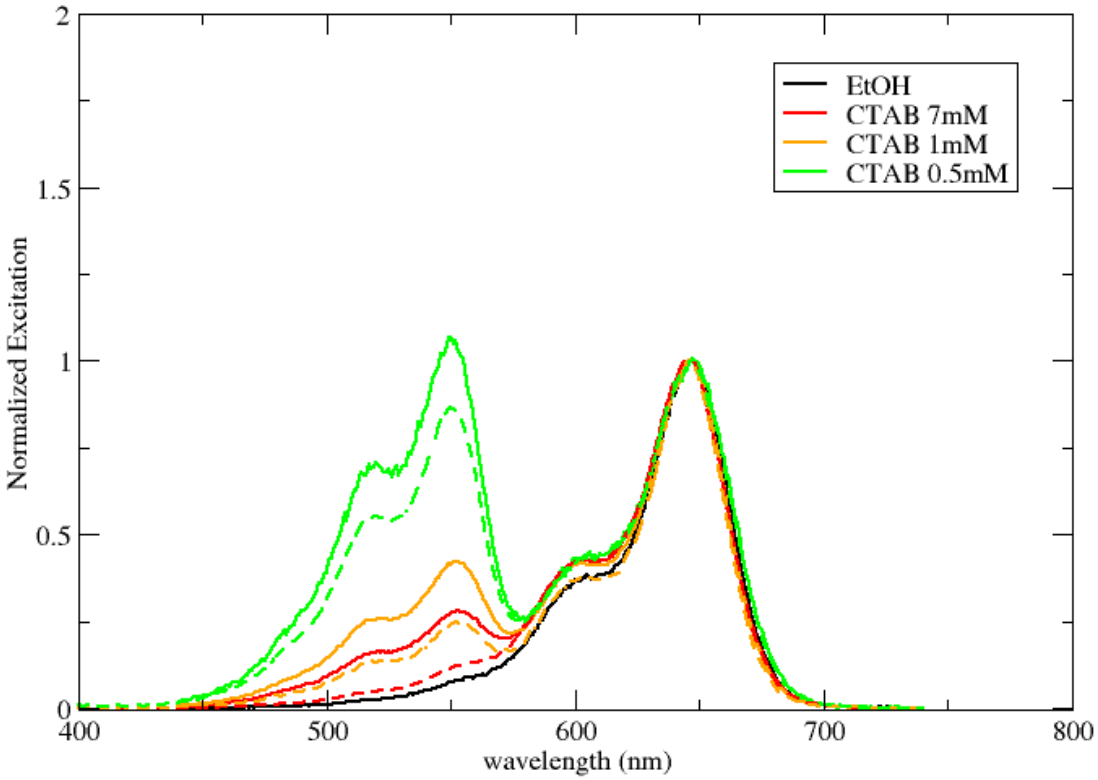

Figure S12: Comparison between excitation spectra of micelles loaded with both DiI and DiD (continuous lines) and mixed micelles of DiI and DiD (dashed lines), collected at 750 nm (emission of the energy acceptor). To minimize inner filter effects, for suspensions at 7 mM, spectra are collected using a cuvette with 1.5 mm optical path.

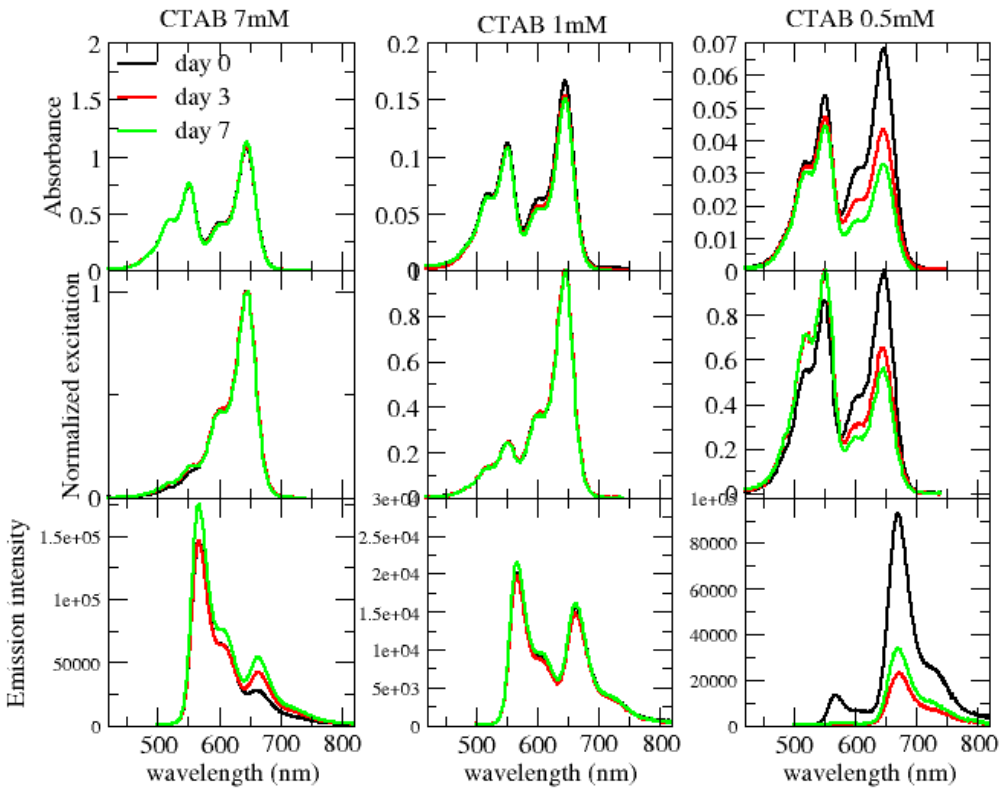

Figure S13: Stability over time of mixed micelles loaded with DiI and DiD for different CTAB concentrations.

MD simulations

Simulating the micelle formation

We performed two simulations of CTAB in water, to promote the formation of micelles. In the first simulation (CTAB1) we introduced 10 CTAB molecules in an $8 \times 8 \times 8$ nm^3 box (concentration 0.032 mol/L). In the second simulation (CTAB90) 90 CTAB molecules were introduced in a $12 \times 12 \times 12$ nm^3 box (concentration 0.086 mol/L). In CTAB10 a single micelle including all CTAB molecules was formed, while in CTAB90 we observe the formation of 10 micelles, each formed by a 4-15 CTAB units (Figure S14).

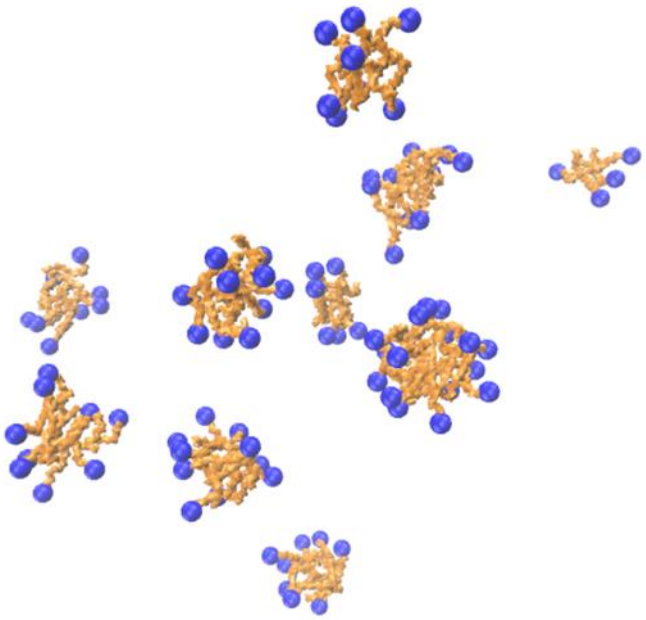

Figure S14: Micelles formed in the CTAB90 simulation (the blue dots correspond to the polar head of each CTAB molecule).

The aggregation number is a concentration dependent parameter. Experimental and computational studies suggest an aggregation number at the CMC, for CTAB micelles, of 60-70[4,5]. The formation of small clusters in our all-atoms MD simulation are ascribed to kinetic effects: while single CTAB molecules are easily incorporated into pre-formed micelles, the subsequent fusion of small clusters is strongly hindered by repulsive interactions between the polar heads of the surfactant. To overcome this issue, a new simulation (CTAB60) was run, starting from a pre-ordered cluster of 60 molecules. This cluster is formed dividing the surface of a sphere into 60 portions of equal area and inserting a CTAB molecule inside each portion, with the long alkyl chain parallel to the sphere radius, as shown in Figure S15 left. This pre-ordered cluster is then solvated and, after a preliminary energy minimization, a 10 ns simulation at constant number of particles, volume and temperature (NVT) is performed. During the simulation, some CTAB units escaped the cluster, forming smaller micelles. However, a micelle containing 42 CTAB units is formed as a stable entity. This micelle is then used to investigate the interaction of the dyes with the micelles (Figure S15 right).

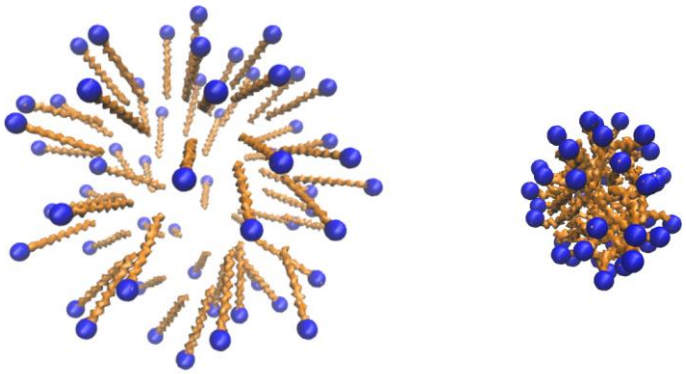

Figure S15: CTAB60 simulation: left, the initial configuration of CT molecules, right the stable micelle formed in the simulation.

Decorating micelles with cyanine dyes

Having formed a stable micelle, we are now in the position to investigate how DiI and DiD enter the micelle. We performed three different experiments: (a) inserting 2 DiI molecules: (b) inserting 2 DiD molecule; (c) inserting 1 DiI and 1 DiD. Each simulation was performed with a first equilibration step followed by a 80 ns NVT simulation, running three replica runs for each sample.

MD Results

In all systems, the electrostatic interaction between the two dyes is calculated in the point-dipole approximation:

$$V = \frac{1}{4\pi\varepsilon_0 r^3}\left[(\vec{\mu}_1 \cdot \vec{\mu}_2) - \frac{3}{r^2}(\vec{\mu}_1 \cdot \vec{r})(\vec{\mu}_2 \cdot \vec{r})\right]$$

where $\vec{\mu}_{1/2}$ is the transition dipole moment associated with each dye, $\vec{r}$ is the intermolecular distance vector and ε_0 is the vacuum dielectric constant. Transition dipole moments are extracted from experimental absorption spectra of the dyes in ethanol. The oscillator strength is a dimensionless quantity obtained from the integrated molar extinction coefficient $\varepsilon(\tilde{\nu})$ follows:

$$f = 4.318 \cdot 10^{-9} \int_0^\infty d\tilde{\nu}\varepsilon(\tilde{\nu})$$

where $\tilde{\nu}$ is the wavevector in cm^{-1}. The oscillator strength is directly related to the transition dipole moment:

$$f = \frac{2m\omega}{3\hbar e^2}|\mu|^2$$

where *e* and *m* are the electron charge and mass, respectively, and ω and μ are the transition frequency and dipole moment, respectively. We obtain *f*=1.05 and μ=11.1 Debye for DiI and *f*=1.39 and μ=13.8 Debye for

DiD. The interchromophore distance was estimated as the distance between the centers of each chromophoric unit, defined as the middle point in the line that in each dye connects the two nitrogen atoms. The same line defines on each dye the direction of the transition dipole moment.

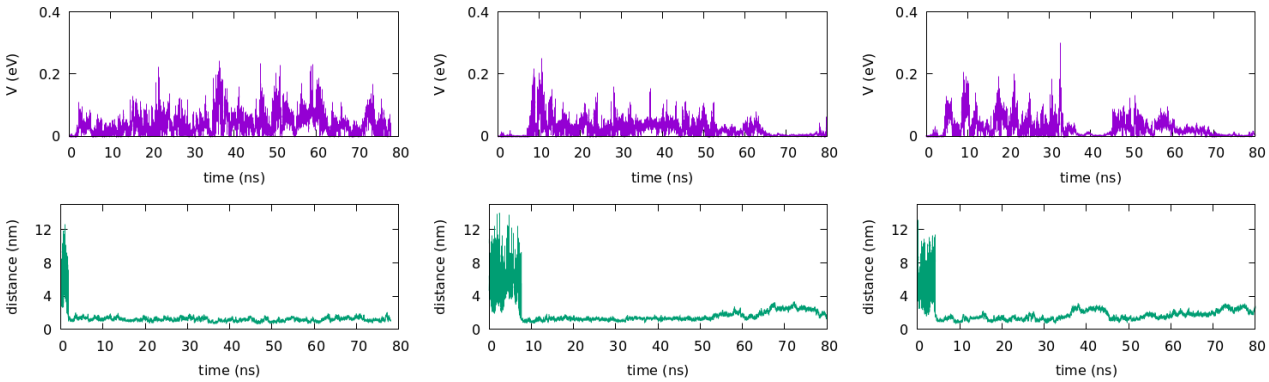

Figure S16: Results from the three simulations run upon addition of two DiI dyes to the CTAB micelle. Green and violet lines refer to the intermolecular distance and the interchromophore interaction (absolute value), respectively. In the simulation on the left panel, the two dyes form a cluster in water that never encounters the micelle.

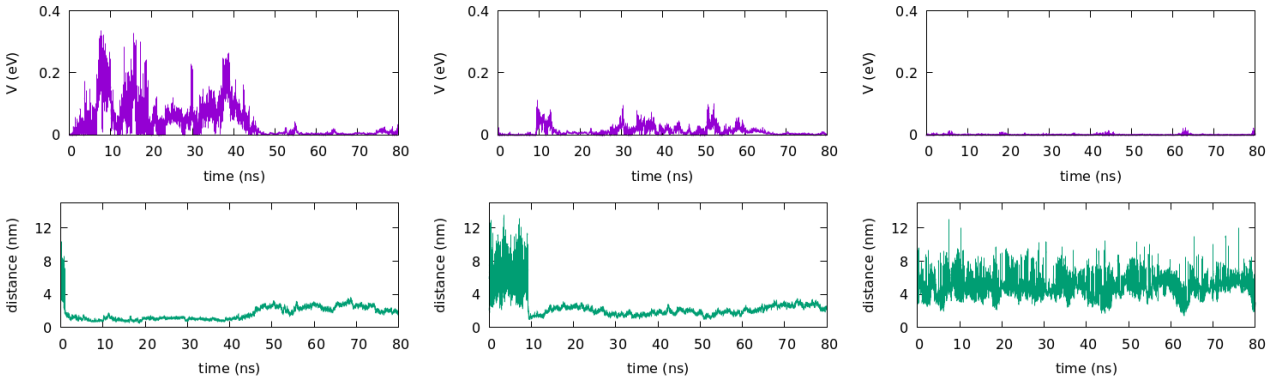

Figure S17: Results from the three simulations run upon addition of two DiD dyes to the CTAB micelle. Green and violet lines refer to the intermolecular distance and the interchromophore interaction (absolute value), respectively. In the simulations in the left and middle panels the two dyes form a cluster in water that then enters the micelle. In the rightmost panel simulation only one dye enters the micelle.

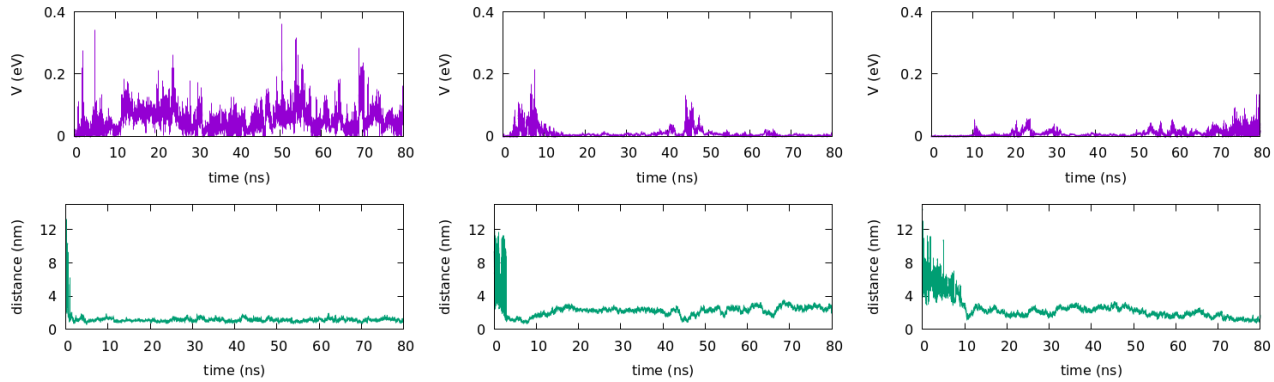

Figure S18: Results from the three simulations run upon addition of a DiI and a DiD dye to the CTAB micelle. Green and violet lines refer to the intermolecular distance and the interchromophore interaction (absolute value), respectively. In all simulations the dyes form a cluster and then enter the micelle.

References

1 V. Patel, N. Dharaiya, D. Ray, V. K. Aswal and P. Bahadur, *Colloids Surfaces A Physicochem. Eng. Asp.*, 2014, **455**, 67–75.

2 R. Dorshow, J. Briggs, C. A. Bunton and D. F. Nicoli, *J. Phys. Chem.*, 1982, **86**, 2388–2395.

3 R. Ragheb and U. Nobbmann, *Sci. Rep.*, 2020, **10**, 1–9.

4 S. Illa-Tuset, D. C. Malaspina and J. Faraudo, *Phys. Chem. Chem. Phys.*, 2018, **20**, 26422–26430.

5 S. P. Moulik, M. E. Haque, P. K. Jana and A. R. Das, *J. Phys. Chem.*, 1996, **100**, 701–708.